

Non-equilibrium Dynamics of Growing Bacterial Colonies

Kai Zhou and Gerhard Gompper

*Institute of Biological Information Processing
Theoretical Physics of Living Matter (IBI-5/IAS-2),
Research center Juelich, Juelich, Germany*

Marc Hennes and Berenike Maier

Institute for Biological Physics, University of Cologne, Cologne, Germany

Benedikt Sabass

*Institute for Infectious Diseases and Zoonoses,
Department of Veterinary Sciences,
Ludwig-Maximilians-Universitaet Munich, Munich, Germany**

Abstract

Colonies of bacterial cells endowed with a pili-based self-propulsion machinery represent an ideal model system for studying how active adhesion forces affect structure and dynamics of many-particle systems. As a novel computational tool, we describe here a highly parallel molecular dynamics simulation package for modeling of *Neisseria gonorrhoeae* colonies. Simulations are employed to investigate growth of bacterial colonies and the dependence of the colony structure on cell-cell interactions. In agreement with experimental data, active pilus retraction is found to enhance local ordering. For mixed colonies consisting of different types of cell types, the simulations show a segregation of cell types depending on the pili-mediated interactions, as seen in experiments. Using a simulated experimental setup, we study the power-spectral density of colony-shape fluctuations and the associated fluctuation-response relation. The simulations predict a strong violation of the equilibrium fluctuation-response relation across the measurable frequency range. Lastly, we illustrate the essential role of active force generation for colony dynamics by showing that pilus-mediated activity drives the spreading of colonies on surfaces and the invasion of narrow channels.

I. INTRODUCTION

Bacterial colonies consisting of cells with nearly identical geometry and mechanical properties are uniquely suited for studying the non-equilibrium statistical mechanics of living matter [1, 2]. A well-established biological model system is the coccoid bacterium *Neisseria gonorrhoeae*. Having a spherical cell body with a diameter of roughly $1\ \mu\text{m}$, the bacterium forms colonies that are reminiscent of nonliving colloidal

* B.Sabass@lmu.de

assemblies. However, bacteria grow and reproduce. Moreover, while colloidal assemblies are held together by passive attractive interactions, *N. gonorrhoeae* colonies are held together by extracellular filaments called type IV pili (T4P) that are cyclically elongated and retracted [3, 4]. T4P are helical polymers consisting mainly of the major subunit PilE. Anchored in a transmembrane-complex, T4P are isotropically displayed on the whole cell surface of *N. gonorrhoeae* [5]. Their elongation and retraction is driven by the dedicated ATPases PilF and PilT, respectively. PilF is required for pilus polymerization and PilT drives pilus retraction and depolymerization of the pilus. During retraction, T4P are capable of generating high forces over 100 pN [6] and the retraction proceeds with velocities up to $2\mu\text{m s}^{-1}$ [1, 5]. When individual cells come into proximity of abiotic surfaces such as glass, cells can attach via T4P. Since *N. gonorrhoea* generates multiple pili simultaneously, a tug-of-war between pili on different sides of the cell body emerges. On glass surfaces, the average detachment force is an order of magnitude smaller than the maximum force generated by pili. Therefore, the tug-of-war leads to a random walk of individual bacteria on surfaces [5, 7–9]. In aerobic environments, individual cells form colonies that are held together by T4P that bind to each other, leading to time-dependent attractive interactions among bacteria [10, 11]. The fact that this interaction is caused by time-dependent non-equilibrium forces affects the shape, dynamics, and sorting behavior of bacterial colonies [7, 15, 16]. *N. gonorrhoea* mutants without T4P or retraction-deficient T4P can not aggregate into colonies [12]. The strength of cell-cell attraction is affected by T4P post-translational modifications and can be controlled by inhibiting or activating different steps of the pilin glycosylation pathway [13]. Mutants with different T4P density and breakage forces spatially segregate inside colonies, suggesting a sorting process driven by a differential of adhesiveness [14, 15].

The material properties of *Neisseria* colonies have been characterized as liquid-like [16] with effective viscosities of $\eta \sim 350 \text{ Pa s}$ for *N. gonorrhoea* [1]. Consistent

with the notion of liquid-like behavior, microcolonies show an effective surface tension. Evidence for an effective surface tension is firstly the spherical shape of microcolonies formed by *N. gonorrhoea* with retractile T4P [17]. Secondly, upon contact, two microcolonies rapidly fuse form a sphere with larger radius as expected for liquid drops [1, 11, 12]. While some material properties of *N. gonorrhoeae* colonies have been characterized, the non-equilibrium effects resulting from active bacterial force-generation remain to be explored. Due to the spherosymmetry of the average force generation by individual bacteria, it may be challenging to distinguish genuine non-equilibrium colony dynamics from dynamics that are also be observable in passive systems. One example is a self-sorting of bacteria inside colonies, where bacteria segregate depending on their activity. Such a segregation has indeed been reported and analyzed [14–16]. Furthermore, it is expected that the active force generation entails a violation of the equilibrium fluctuation-response theorem [18–22]. One aim of this work is to establish a few theoretical predictions regarding the non-equilibrium fluctuations of *N. gonorrhoeae* colonies.

The study of physical properties of large bacterial colonies requires computer simulations. Previous work includes simulations of the dynamics of single cells due to individual pili [5] and coarse-grained approaches or continuum theories for describing *Neisseria* colonies [23]. Furthermore, multiscale simulations combining overdamped cell dynamics with stochastic pilus activity have shown great promise in studies of the behavior of *Neisseria* colonies on different lengthscales [9, 16]. Mechanical forces in bacterial cell colonies are not only caused by T4P retraction but also result from cell growth and division. For the case of mammalian cells, tissue growth has been studied extensively with particle-based simulations where individual cells are represented as spheres [24, 25]. The sphericity and growth dynamics assumed for cells with these models are also appropriate for simulating coccoid bacteria.

The present work is based on a new code for multiscale simulation of colonies

consisting of coccoid bacteria that employ T4P to generate active forces while also growing and dividing. We employ here the highly parallel, classical molecular dynamics code LAMMPS and add a dedicated package for simulation of growing cells that interact with each other through elastic, retractable bonds representing pili. Using this model, we simulate the growth dynamics of colonies and the structural order of cells inside colonies. With appropriate parameterization, the simulation results are consistent with experimental findings. Simulations results for cell segregation in colonies consisting of different mutants of the T4P machinery are in agreement with experimental results. Furthermore, we predict a measurable violation of the equilibrium fluctuation-response theorem for fluctuations of the colony shape and we show that a colony invasion of narrow channels is driven by active pilus-mediated forces.

This article is organized as follows. We introduce the theoretical background and computational model in Sec. II. Bacterial growth and colony formation are investigated in Sec. III A. Next, the local ordering of bacteria and its dependence on active force generation is studied in Sec. III B. Simulation results for the occurrence of segregation in mixed bacterial colonies are provided in Sec. III C. Fluctuations of the colony shape are studied in Sec. III D, where we also predict a violation of the equilibrium fluctuation-response theorem as a result of the time-dependent pilus-retraction forces. Results for the interaction of colonies with surfaces and channels are given in Sec. III E. A few concluding remarks are made in Sec. IV.

II. SIMULATION OF COLONIES OF COCCOID CELLS

In our simulations, colonies are grown from individual cells through cell division. An individual cell is also called a coccus. A pair of dividing *N. gonorrhoeae* cells is called a diplococcus and has the shape of two partially overlapping spheres. During

the growth, each diplococcus divides approximately with rate α into a pair of individual cocci, which in turn again become diplococci after some time. Each individual coccus is endowed with a repulsive potential modeling volume exclusion. In addition, cells experience dissipative forces resulting from relative motion of neighboring cells and thermal fluctuations. Each cell has several pili. By modeling the pili as dynamic springs that can extend, retract, bind and unbind either with other pili or with the environment, we faithfully represent the stochastic nature of cell-generated forces.

A. Cell geometry and bacterial growth

Individual cells are modeled as soft spheres with radius R . The position of the center of bacterium i is denoted by \mathbf{r}_i . The vector between a pair of bacteria with indices (i, j) is denoted by $\mathbf{r}_{ij} = \mathbf{r}_i - \mathbf{r}_j$ and their distance is $r_{ij} = |\mathbf{r}_{ij}|$.

The division of a cell with index i is modeled by insertion of a second sphere with index j on top of i . The pair of cells is initially connected by an elastic spring with time-dependent rest length $l(t)$, thus forming a diplococcus. The initial orientation of the vector connecting the cell pair is chosen randomly. Then, growth of the diplococcus is simulated by increasing the rest length of the spring that connects the cell pair as

$$\frac{dl(t)}{dt} = \frac{\alpha}{\nu_r}, \quad (1)$$

where $1/\nu_r$ is a constant with units of length. Once the length $l(t)$ reaches a threshold denoted by l_t , the connecting spring is removed and the two spheres are treated as individual cocci. Instantaneous forces acting on either of the two cocci during their separation are equally distributed among the two cocci to ensure momentum conservation. The time between creation of a diplococcus and separation of the two daughter cells is given by $t_r = l_t \nu_r / \alpha$.

After separation of a diplococcus, the two individual cocci do not become diplococci instantaneously. Rather, individual cells are turned into diplococci at a constant rate per cell α . This means that the separation of a diplococcus (division) is followed by a random refractory time, which prevents an unphysical synchronization of the division events in the simulations.

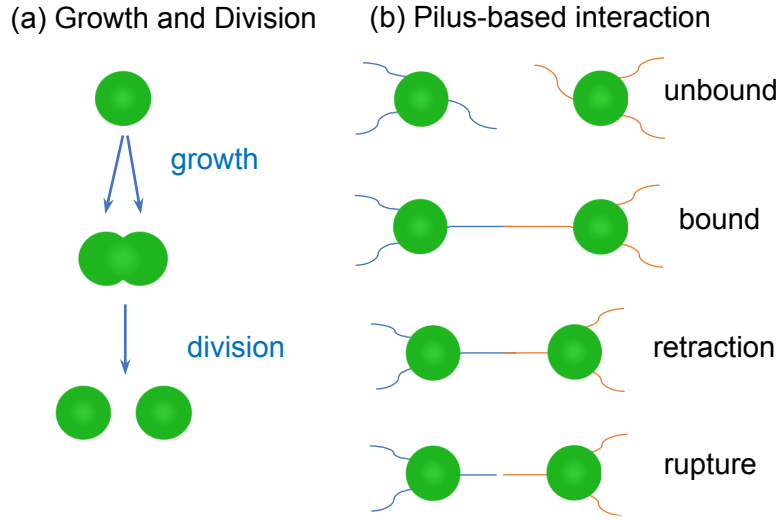


FIG. 1. Schematic representation of the two active processes occurring in the simulations: (a) A bacterium grows into a diplococcus and then divides into two individual bacteria. (b) Two cells bind to each other via pili. Subsequently, pili are retracted by the bacteria leading to a force build-up. The bond connecting the pili ruptures stochastically in a force-dependent manner.

B. Dynamics of type-IV pili

Each cell is assumed to have a constant number of pili, typically up to 25. A pilus of bacterium i is assumed to bind with a rate k_{bind} to one pilus of a neighboring

bacterium j . For binding, the distance between i and j , r_{ij} , is required to be less than a cutoff distance d_{bind} . This cutoff distance ensures that only bacteria bind to each other when they are in proximity to each other. In some simulations, a Voronoi triangulation is used to limit pilus interactions only to closest neighbors. For simplicity, we assume that pilus-based forces act along the straight lines connecting the centers of cell pairs. It is assumed that two bacteria can only have one pair of pili adhering to each other. Likewise, bundling of pili [5] is also neglected due to its unknown role in cell colonies. Pili of the two cells in a diplococcus do not bind to each other. The pilus-based cell-cell connection is modeled as a spring connecting the centers of two cells. The rest length of the pilus spring connecting two cells with indices i and j is denoted by L_{ij} and the force exerted between the pair of cells has a magnitude of

$$f_{ij}^p = -k[r_{ij}(t) - L_{ij}(t)], \quad (2)$$

where k is the pilus' spring constant. Once the pilus is bound, it is assumed to retract. Pilus retraction leads to a continuous shortening of its rest length as

$$L_{ij}(t) = r_{ij}(0) - \int_0^t v_{\text{re}}(t) dt, \quad (3)$$

where v_{re} is the force-dependent retraction velocity of pili. To describe the force-velocity relationship for T4P retraction motors [6], we employ the following linear approximation

$$v_{\text{re}}(t) = \max \left[0, v_{\text{re}}(0) \left(1 - \frac{f_{ij}^p}{f_s} \right) \right], \quad (4)$$

where the stall force f_s represents the maximal force a retracting pilus can generate. Furthermore, it is assumed that the bonds between the pili rupture under stress with a force-dependent rate as

$$\gamma_{\text{rupt}} = k_{\text{rupt}} e^{F_{ij}^p / F_{\text{rupt}}}, \quad (5)$$

where k_{rupt} is pilus rupture rate without loading and F_{rupt} is characteristic rupture force.

C. Dynamics of bacteria

For simulating the dynamics of cells, we employ an algorithm similar to dissipative particle dynamics (DPD), where we assume a soft repulsion between cells, frictional force proportional to the relative velocity of neighboring cells, and thermal noise forces satisfying the Einstein relation. Underdamped equations of motion for every cell i with mass m_i , position \mathbf{r}_i , velocity \mathbf{v}_i , and force \mathbf{f}_i are assumed as

$$\frac{d\mathbf{r}_i}{dt} = \mathbf{v}_i, \quad m_i \frac{d\mathbf{v}_i}{dt} = \mathbf{f}_i. \quad (6)$$

The force acting on each pair of cells consists of conservative forces \mathbf{F}_{ij}^c , dissipative forces \mathbf{F}_{ij}^d , thermal fluctuations \mathbf{F}_{ij}^r and forces from active pilus retraction \mathbf{F}_{ij}^p .

Overall, the sum of these forces is

$$\mathbf{f}_i = \sum_{j \neq i} (\mathbf{F}_{ij}^c + \mathbf{F}_{ij}^d + \mathbf{F}_{ij}^r + \mathbf{F}_{ij}^p). \quad (7)$$

For defining the individual force terms, we employ the vector between the centers of masses $\mathbf{r}_{ij} = \mathbf{r}_i - \mathbf{r}_j$ and the unit vector pointing towards cell i denoted by $\hat{\mathbf{r}}_{ij} = \mathbf{r}_{ij}/r_{ij}$.

The conservative force for a pair of unbound bacteria is given by

$$\mathbf{F}_{ij}^c = \begin{cases} a_0(1 - r_{ij}/d_{\text{con}})\hat{\mathbf{r}}_{ij} & (r_{ij} < d_{\text{con}}) \\ 0 & (r_{ij} \geq d_{\text{con}}) \end{cases}, \quad (8)$$

where a_0 is the maximum conservative force between bacterium i and j , the cutoff distance for the repulsive cell-cell interaction is denoted by $d_{\text{con}} = 2R$. For a diplococcus consisting of two spheres, the conservative force due to growth is

$$\mathbf{F}_{ij}^c = a_{\text{growth}}(l_i - r_{ij})\hat{\mathbf{r}}_{ij}, \quad (9)$$

where a_{growth} is the elastic constant of the spring connecting the two cells of a diplo-

coccus. The dissipative and random forces are, respectively, given by

$$\mathbf{F}_{ij}^d = -\gamma\omega^D(r_{ij})(\hat{\mathbf{r}}_{ij} \cdot \mathbf{v}_{ij})\hat{\mathbf{r}}_{ij}, \quad (10)$$

$$\mathbf{F}_{ij}^r = \sqrt{2\gamma k_B T}\omega^R(r_{ij})\theta_{ij}\hat{\mathbf{r}}_{ij}, \quad (11)$$

where γ is a friction coefficient, ω^D and ω^R are distance-dependent weight functions, k_B is the Boltzmann constant, T is the ambient temperature and $\theta_{ij} = \theta_{ji}$ is a random number drawn from a Gaussian distribution with zero mean and unit variance. For the distance-dependence of the friction force we choose

$$\omega^D(r) = [\omega^R(r)]^2 = \begin{cases} (1 - r_{ij}/d_{\text{dpd}})^2 & (r_{ij} < d_{\text{dpd}}) \\ 0 & (r_{ij} \geq d_{\text{dpd}}) \end{cases}, \quad (12)$$

where d_{dpd} is the cutt-off for dissipative and random forces. Finally, the forces resulting from retraction of pili are given in their vectorial form by

$$\mathbf{F}_{ij}^p = f_{ij}^p \hat{\mathbf{r}}_{ij}. \quad (13)$$

D. Simulation details and parameter values

The simulation code is integrated into the molecular dynamics code LAMMPS [26], which allows an efficient parallelization of the code while providing great flexibility regarding the model choice. To model the cellular dynamics described above, we wrote a new C++ package. The velocity-Verlet algorithm is used to advance the set of positions, velocities and forces. The code is parallelized for execution on CPUs and large colonies consisting of ten-thousands of bacteria can be simulated efficiently. The colonies are visualized with OVITO [27].

The characteristic scales that are used as simulation units are the cell diameter $d_c = 2R = 1\ \mu\text{m}$, a timescale given by the inverse of the default value of the pilus-unbinding rate constant $t_c = 1/k_{\text{rupt}} = 1\text{ s}$, and a force scale of $f_c = 1\ \text{pN}$. Parameters

TABLE I. The choice of parameters for simulations.

Parameter	Value	Unit	Reference
cell radius R	0.5	d_c	[1]
pilus spring constant k	2000	$f_c d_c^{-1}$	[28]
pilus stall force f_s	180	f_c	
maximum retraction velocity of pili v_0	2	$d_c t_c^{-1}$	
number of pili per cell	7		[8]
simulation time step Δt	$1 \times 10^{-4} t_c$		
division rate α	1/1500	t_c^{-1}	
diplococcus growth parameter ν_r	1.0	d_c^{-1}	
pilus rupture rate k_{rupt}	1	t_c^{-1}	
pilus binding cutoff distance d_{bind}	2.5	d_c	
pilus binding rate k_{bind}	10	t_c^{-1}	
pilus-pilus bond rupture force scale F_{rupt}	60	f_c	[1, 14]
maximum conservative force a_0	4000	$f_c d_c^{-1}$	
conservative force cutoff $d_{\text{con}} = 2R$	1.0	d_c	
diplococcus spring constant a_{growth}	4000	$f_c d_c^{-1}$	
friction coefficient γ	2000	$f_c t_c d_c^{-1}$	
thermal energy scale $k_B T$	$1 \times 10^{-6} f_c d_c$		
dissipative and random force cutoff d_{dpd}	1.5	d_c	

values that are used for the simulations are listed in Tab. I. Whenever alternative parameter values are used, they are listed with the results.

E. Separation of time scales

In the simulations, the time scale of viscous relaxation is smaller than the time-scale of pilus-based interaction. Thus, inertial effects are negligible. Moreover, the time scale of the pilus-based interaction is much smaller than the time-scale of cell division $t_c \ll 1/\alpha$. Simulations typically start with one bacterium and colonies are formed by letting the cells grow and divide. The colony structures emerge during growth due to the repulsive interactions, thermal noise, and pilus-based interactions, as shown in Fig.2(a). In some simulations, it is desirable to completely remove the effect of cell growth on the bacterial dynamics. For this purpose, cell growth and division are switched off after a sufficient colony size is reached.

III. RESULTS

A. Colony growth

Figures 2 shows simulation results for colony growth. As for experimental systems, colonies approximately maintain a spherical shape during growth. In the simulations, both the number of bacteria and the colony radius increase exponentially with time. Since we have not taken into account a position-dependence of nutrient availability inside colonies, we expect to see such growth dynamics only for small cell colonies in rich media. Experimentally, it has been observed that the radius of young *N. gonorrhoeae* colonies grows exponentially for approximately three hours [29].

Next, analytical formulas are derived for the simulated growth dynamics. The cell-growth simulations are based on the assumption of two growth phases - consisting of single cocci and diplococci- that have been adopted for computational convenience. The advantage of this two-phase model is that it allows one to introduce a controllable

randomization of division events and to thus avoid artificial division synchronization in simulations. A single coccus can divide to form a diplococcus and this is a random event that occurs with rate α . The resulting diplococcus can not divide immediately but grows on average for a time t_r until it separates into two single cocci that can then divide. We denote the average number of all cells forming the cocci and diplococci by $N(t)$. The average number of cells that are single cocci is denoted by $N_c(t)$. Since only the single cocci are assumed to divide, the overall number of bacteria is determined by

$$\frac{dN(t)}{dt} = N_c(t)\alpha. \quad (14)$$

We next consider the governing equation for the number of single cocci $N_c(t)$. The number of single cocci increases at time t through separation of diplococci. The separating diplococci, in turn, were formed at time $t - t_r$ through division of single cocci. Hence, the increase of single cocci at time t is given by $2\alpha N_c(t - t_r)$, where the factor 2 results from cell-doubling during division. Simultaneously, the number of single cocci is reduced through formation of diplococci with rate $\alpha N_c(t)$. Overall, we have

$$\frac{dN_c(t)}{dt} = 2\alpha N_c(t - t_r) - \alpha N_c(t). \quad (15)$$

Growth is assumed to obey an exponential time-dependence and the Ansatz $N_c(t) = N_c(0)e^{\alpha p t}$ with a new constant p is inserted into Eq. (15). This yields a nonlinear equation determining p as

$$p = 2e^{-p\alpha t_r} - 1. \quad (16)$$

Insertion of this result into Eq. (14) yields the final result for the overall cell number as

$$N(t) = N_c(0)e^{\alpha p t}/p. \quad (17)$$

Thus, the effective growth rate of the cell number in simulations is given by αp . Formula (17) has no free parameters and fits to the simulation results, see the inset

of Fig. 2(c).

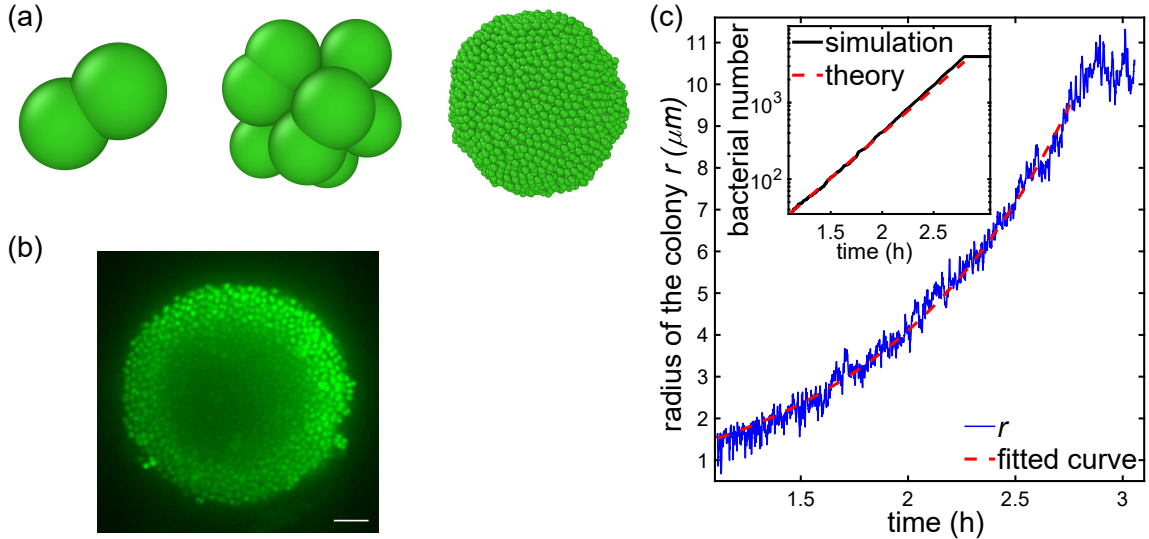


FIG. 2. (a) Simulation snapshots showing colony formation. (b) Confocal section of a *N. gonorrhoeae* colony. Scale bar: $10\ \mu\text{m}$. (c) Cell numbers and colony radii increase exponentially with time in the simulations.

B. Pilus-mediated interactions determine local colony order

To establish that the parameter values chosen for simulating pili correspond to measured values for *N. gonorrhoeae*, the distributions of rupture forces in our simulations are recorded and compared with experimental results, see Fig. 3(a). The cell density plays a role for a colony's viscoelastic material properties and its apparent surface tension. In the simulations, the number density of cells depends on the balance of the repulsive potential forces and the pilus retraction forces. Figure 3(c) shows the mean number density as a function of the distance from the colony center. While the density is approximately constant inside colonies, it drops off at their

perimeters. Increasing the cutoff for pilus-based cell-cell interaction leads to denser colonies.

Next, the local order in simulated colonies is investigated. The degree of local ordering is characterized by the radial distribution function (RDF), which is the average local particle density at distance r from any reference particle, normalized by the average particle density of the system [30, 31]. The RDF is defined as

$$g(r) = \frac{\sum_{i=1}^N \phi_i(r)/(NV_{\text{shell}}(r))}{N/V}, \quad (18)$$

where $\phi_i(r)$ is the number of particles whose distance to the i th particle is between $r - \Delta r$ and $r + \Delta r$ with $\Delta r = 1$, $V_{\text{shell}}(r)$ is the volume of the shell between radii $r - \Delta r$ and $r + \Delta r$, N is the total number of particles in the system, and V is the volume of the colony. Figure 3(d) contains plots of the RDFs of bacteria inside stationary, non-growing colonies. For bacteria carrying few pili, the structure is rather disordered as shown by the nearly monotonous decrease of the RDF for $r > d_c$. For cells carrying 7 – 25 pili, which corresponds to the experimentally established number for wild-type *N. gonorrhoeae*, the RDFs have the typical characteristics seen for liquids with multiple, decreasing maxima. Hence, pilus-based cell-cell interaction generates structures with near-range order. Since the pili also cause relative motion of the bacteria, decreasing pilus retraction speed increases the spatial ordering as seen in Fig. 3(e). During growth, the distances between two cocci in a diplococcus are smaller than the average cell radius, which leads to the appearance of an additional peak in the RDF, which fades away once growth and division have stopped, see Fig. 3(f).

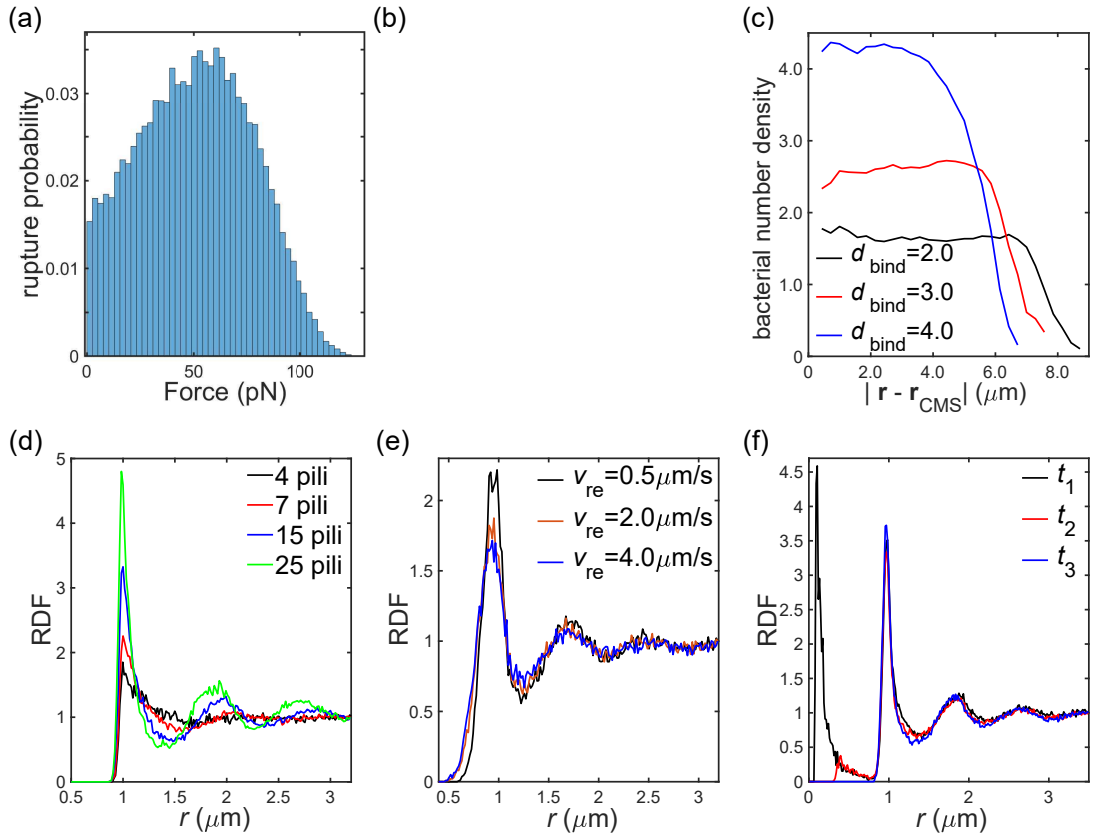


FIG. 3. (a) Distribution of pilus-pilus bond rupture forces simulations (b) Experimental results for the distribution of pilus-pilus bond rupture forces measured with an optical trap. (c) Number density of cells as a function of distance from the colony center in simulations. The cutoff range d_{bind} for formation of a pilus bond between two cells significantly affect the cell density. (d) Radial distribution function (RDF) of cells in simulated colonies. Decaying maxima result from a local, liquid-like order. The maxima in the RDF appear with increasing numbers of pili per cell, indicating that pili numbers determine a transition from a disordered gas-like phase to a liquid-like phase. (e) RDF inside simulated colonies for different pilus retraction velocities. (f) RDF inside colonies during growth. At t_1 , cells are growing as diplococci and dividing. The additional maximum at short distances results from small distances between individual cells in diplococci. At t_2 , division stopped while growth of diplococci continues. At t_3 , growth and division have both been stopped. $d_{bind} = 2.0 \mu\text{m}$

C. Active phase segregation in mixed colonies

Experimentally, it has been found that strains carrying mutations affecting the T4P machinery segregate during formation of colonies [14, 15]. Bacterial segregation was seen to be dependent on the number of pili per cell, on post-translational pilus modifications that modify binding properties, and on the ability of bacteria to retract their pili. The observed colony morphotypes were suggested to be in agreement with the so-called differential strength of adhesion hypothesis, which proposes that contractive activity of cells in addition to differential adhesiveness drives cell sorting. While active force generation was seen to be necessary for defined morphologies of mixed microcolonies, an experimental separation of the effect of pilus activity from differential adhesiveness is challenging due to the molecular complexity of pili. Simulations allow one to study how variation of different parameters affects segregation.

To establish that the simulations produce results that are consistent with experimental data, experimentally studied cases of colony segregation are re-investigated. We first simulate simultaneous growth of two kinds of strains carrying different numbers of pili, as studied experimentally in Ref. [14]. In simulations, the growing colonies segregate and the cells that have many pili concentrate in the center of the colony while cells with fewer pili form a spherical shell in the periphery, see Fig. 4(a). Qualitatively, this configuration can be explained by the hierarchy of interaction strengths, as explained in Ref. [14]. The mutual attraction of a pair of cells with many pili is larger than the attraction of a cell with many pili to a cell with few pili. The weakest attraction occurs among pairs of cells with few pili. The formation a shell of weakly-binding cells in the periphery is energetically advantageous because of the gain in surface energy. For binary mixtures of bacteria with different pilus-rupture probabilities, other hierarchies of interaction strength are possible. For

a mixture of two cell-types that have high pilus-rupture forces among each other, but lower rupture forces for pairs of different cells, simulations show the formation of two segregated half-spheres during growth, see Fig. 4(b). This is consistent with experimental results for where wild-type cells were mixed with mutants deficient in post-translational pilin glycosylation [14].

Previous work on pilus-driven self-assembly of colonies has shown that binary cell mixtures consisting of cells with intact and retraction-deficient pili segregate [9, 15]. To learn more about the segregation dynamics in this case, we start our simulations with fully grown colonies consisting of random binary cell mixtures, see Fig. 4(c). Half of the cells can retract their pili and the other half are retraction-deficient. Since both cell types have the same number of pili, no differential in adhesiveness exists. Nevertheless, the initially random distribution of different cell types gradually disappears and the retraction-deficient cells accumulate at the periphery of the simulated colony, as found in Ref. [9]. Unexpectedly, our simulations also predict the existence of a metastable intermediate state, in which actively retracting cells form a concentric spherical shell inside the colony, see Fig. 4(c, t_3). The lifetime of the predicted intermediate state depends on the pilus-based interactions and on the strength of the cell-cell repulsion. We quantify the effect of pilus retraction velocity and cell-cell repulsion on the appearance of the metastable concentric shell. Heat-maps of the average lifetimes of the concentric spheres as a percentage of the simulation time are shown in Fig.4(d). For short-ranged pilus interactions, the concentric shell of retracting cells inside the colony hardly appears, see Fig.4(d, i), ($d_{\text{bind}} = 2$). Likewise, this metastable state is suppressed if pilus-mediated interactions are limited to the next neighbors via Voronoi triangulation. The appearance of the metastable state requires long-ranged pilus-pilus interactions and rather stiff repulsive potentials among cells, see Fig.4(d, ii) ($d_{\text{bind}} = 3$). Through such long-ranged pilus-pilus interactions, cells can exert forces on other cells that are not their direct neighbors. The

simulations suggest that a experimental observation of a metastable concentric shell during phase separation could potentially point toward the existence of long-ranged, pilus-based interactions among bacteria.

Figure 4(e, i) shows plots of the mean diffusion coefficient of cells as a function of the distance from the colony center. First, cell colonies consisting of one cell type are considered. Consistent with experimental results and previous computational work,[15, 32] diffusive motion of cells decreases at the center of the colonies. These gradients in mobility are not a result of graded mechanical activity because all cells in the simulations have the same properties. For segregated colonies consisting of cells with retracting and non-retracting pili, the diffusion constant decreases with the distance from the colony center. This position-dependence of the cell mobility is consistent with the increasing concentration of pilus-retraction deficient cells at the periphery of the colony, see Fig.4(e, ii).

D. Non-equilibrium fluctuations of colony boundaries

The position fluctuations of cells in colonies on the one hand provide information about the viscoelastic properties of the system and on the other hand carry information about the non-equilibrium forces holding the system together. While it is trivial to keep track of cell positions in simulations, experimentally, it is a great challenge to measure the position of the cells inside a three-dimensional colony with high spatio-temporal precision. However, it is possible to image whole colonies with high frame rate and subsequently extract the colony edges from the images. Thus, the non-equilibrium fluctuations of colony boundaries are observable. We simulate here such a measurement by tracking cells located in a fixed small sector at the edge of colonies in the stationary state, as shown in Fig.5(a). In this setup, a movement of bacteria at the colony edge can either result from thermal noise or the activities

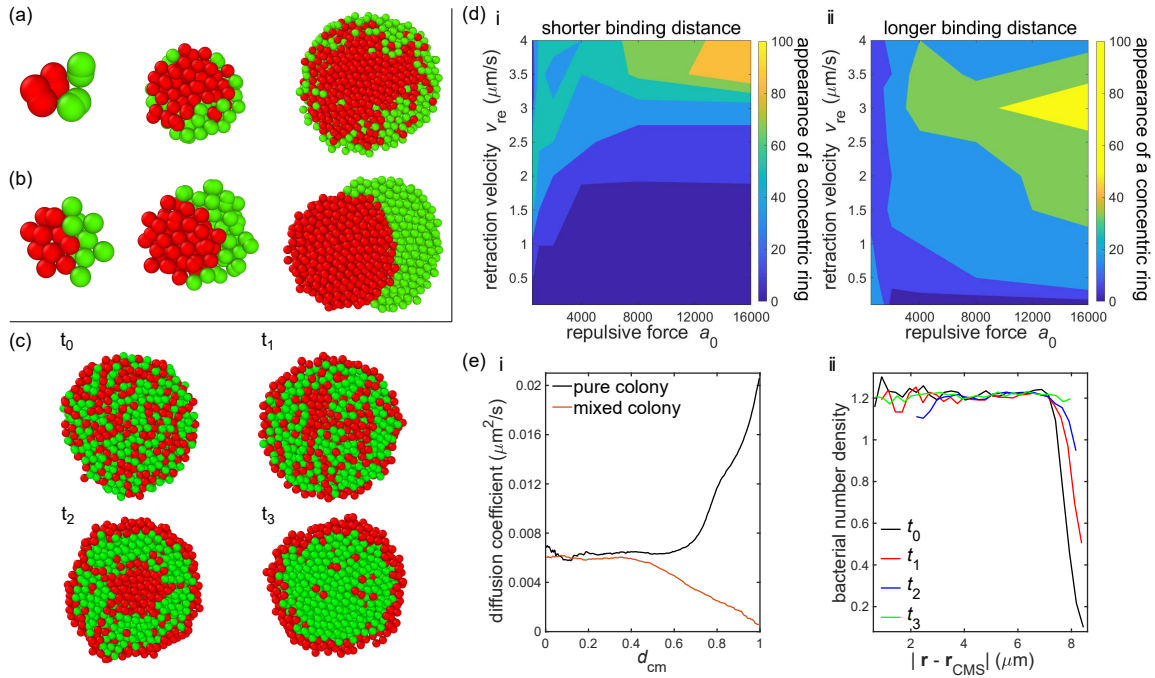


FIG. 4. Phase segregation of mixed colonies. (a) Growing colony consisting of cells with 14 pili (red) and cells with 7 pili (green). (b) Simulated growth of a mixture of wild-type cells (WT, green) and mutants deficient in post-translational pilin glycosylation (GD, red) [14]. Pilus rupture forces are as follows: $F_{\text{rupt}}^{\text{WT-WT}} = 60 \text{ pN}$, $F_{\text{rupt}}^{\text{GD-WT}} = 30 \text{ pN}$, $F_{\text{rupt}}^{\text{GD-GD}} = 36 \text{ pN}$. In (a) and (b), Voronoi triangulation is used to locate neighbors for pilus binding. (c) Segregation of a binary mixture of wild-type bacteria (green) and pilus-retraction-deficient cells (red). Pilus-mediated interactions are long-ranged in this example with $d_{\text{bind}} = 2.5 \mu\text{m}$. At t_0 , the colony is randomly mixed. Over time, the proportion of pilus-retraction-deficient cells increases in the colony periphery, t_1 , and wild-type cells then accumulate in a concentric sphere inside the colony, t_2 . The concentric sphere eventually disappears and wild-type cells accumulate in the colony center, t_3 . (d, i) Lifetime of the concentric sphere arrangement for short-ranged pilus interactions, $d_{\text{bind}} = 2.5 \mu\text{m}$. Lifetimes are given in percent of the longest observed lifetime (3000s). (d, ii) Lifetime of the concentric sphere arrangement for long-ranged pilus interactions, $d_{\text{bind}} = 3.5 \mu\text{m}$. Lifetimes are given in percent of 3000 s. (e, i) Diffusion coefficients of individual cells in a colony as a function of the normalized radial distance from the colony center, d_{cm} . Pure colonies consist of one type of cells, the mixed colony is the segregated system shown in (c, t_3). (e, ii) The mean radial number density of wild-type cells (green) for the simulation snapshots shown in (c).

of pili. Colonies are grown in simulations using wild-type cells. After switching off colony growth, the role of pilus activity for the stationary state is studied. The decay time of the velocity autocorrelation function (VACF) in stationary state without active pilus-mediated forces, $v_{\text{re}} = 0$, corresponds to the inertial timescale in simulations. Roughly, we thus have an inertial decay time $t_{\text{inert}} \simeq 0.1 k_{\text{rupt}}^{-1}$ (simulation units), see Fig.5(b). The cell motion resulting from pilus retraction strongly increases the VACF below the timescale of pilus-bond rupture $k_{\text{rupt}}^{-1} = 1 \text{ s}$.

Denoting the radial distance between the center of mass and the edge of the colony by $r_{\text{CMS}}(t)$, the deviations from the time average are given by $X(t) = (r_{\text{CMS}}(t) - \langle r_{\text{CMS}} \rangle)$. The power spectral density (PSD) of the displacement is given by

$$P(\omega) = \frac{|\tilde{X}(\omega)|^2}{s n}, \quad (19)$$

where $\tilde{X}(\omega)$ is the discrete Fourier transform of $X(t)$, s is the sampling rate, and n is the number of data points. The PSDs of the radial motion of bacteria at the boundary in our simulated colonies are shown as Fig.5(c). Fluctuations with frequencies $\omega \lesssim 10 \text{ Hz}$ are expected to be experimentally accessible. For $\omega > 2\pi/t_{\text{inert}} \simeq 50 \text{ Hz}$, the results are not expected to match with experiments since here inertial effects start to play a role the in simulations.

First, retraction deficient, passive pili with $v_{\text{re}} = 0$ are considered. Since these pili only form temporary, rupturing bonds between the cells, they produce an effective friction among cells. The boundary fluctuation are similar to the motion of an overdamped particle in a purely viscous environment $P(\omega) \propto \omega^{-2}$. Second, we consider the case of retraction deficient, passive pili that form permanent bonds ($v_{\text{re}} = 0$, no rupture). Here, boundary fluctuation are similar to the motion of an overdamped particle in an harmonic potential with $P(\omega) \propto \text{const.}$ at low frequencies. Third, we consider wild-type cells with retracting T4P. Pilus retraction on the one hand enhances the elastic forces among cells and, on the other hand, also increases the

rupture rate of bonds formed by T4P. Therefore, the PSD of boundary fluctuations for wild-type cells lies between the limiting cases of purely viscous and visco-elastic materials. Experimental measurement of colony boundary fluctuations up to 10 Hz are in qualitative agreement with our simulation results but some deviations from expected viscous response $P(\omega) \propto \omega^{-2}$ at high frequencies are observed, possibly because of the limited sampling rate in experiments.

Since shape fluctuations of a wild-type cell colony mainly result from active forces, a violation of the equilibrium fluctuation-response relation is expected. To find out how a fluctuation-response relation can be measured experimentally, we simulate a setup for controlled mechanical perturbation of the colony boundary. We fix a simulated colony between walls and stick a bead with radius $R_B = 1.5 \mu\text{m}$ onto one side of the colony, see Fig. 5(d). The same parameter values are used to describe pilus interaction with walls and pilus-pilus interaction. The pairwise interactions between the bead and the cells is modeled with a Morse potential. Denoting the distance between the bead and any neighboring cell i by $r_{i,B}$, the potential is given by

$$\Psi_i^B(r_{i,B}) = c_{\text{mors}} [e^{-2\beta(r_{i,B}-R_{i,B})} - 2e^{-\beta(r_{i,B}-R_{i,B})}], \quad \text{for } r_{i,B} \leq d_{\text{mors}}, \quad (20)$$

$$\Psi_i^B(r_{i,B}) = \Psi_i^B(d_{\text{mors}}), \quad \text{for } r_{i,B} > d_{\text{mors}}, \quad (21)$$

where sum of the radii of cell and beads is given by $R_{i,B} = R + R_B$. The cutoff for the interaction potential is set at $d_{\text{mors}} = 2.7 \mu\text{m}$. Other parameter values of the potential are fixed as $c_{\text{mors}} = 40 \text{ pN}\mu\text{m}$ (energy unit: $f_c d_c$) and $\beta = 1 \mu\text{m}^{-1}$. The radial displacement of the bead relative to the center of the colony, $x(t)$, is employed to quantify the fluctuations of the colony boundary through a PSD $P(\omega)$ given by Eq. (19). Alternatively, a sinusoidally varying force $F_{\text{ext}}(t)$ is applied to the beads' center, pointing towards the colony center. The Fourier transform of the force is

given by $\hat{F}_{\text{ext}}(\omega)$ with angular frequency ω . The response function is given by

$$\hat{\chi}(\omega) \equiv \frac{\hat{x}(\omega)}{\hat{F}_{\text{ext}}(\omega)}. \quad (22)$$

Denoting by $\hat{\chi}'(\omega)$ the imaginary part of the response function $\hat{\chi}(\omega)$, we define the quantity $H(\omega) \equiv -\hat{\chi}'(\omega)2k_B T/\omega$. For systems in thermal equilibrium, the fluctuation-response theorem states that

$$P(\omega) = H(\omega). \quad (23)$$

For colonies consisting of bacteria with retraction-deficient, passive pili and permanent bounds ($v_{\text{re}} = 0$), Eq. (23) is satisfied and the the fluctuation-response theorem holds as expected, see Fig. 5(e). In simulations of colonies consisting of wild-type bacteria that can retract their pili ($v_{\text{re}} = 0.5 \mu\text{m/s}$) and form dynamic bonds with other cells, the equilibrium fluctuation response relationship is violated across the whole experimentally relevant frequency range of $[0 - 10] \text{ Hz}$. Moreover, the simulations predict a very strong deviation from Eq. (23), where $P(\omega)$ is several magnitudes larger than $H(\omega)$. Such deviations are likely measurable in experiments.

E. Active colony spreading and invasion of narrow channels

As a further application of our simulation framework, we consider the interaction of colonies with soft walls that provide attachment sites for pili. Walls are represented by immobile soft spheres. Cell-wall interactions are represented by the same conservative potential leading to cell-cell repulsion. Since biomolecular binding affinities are typically determined by the unbinding rate, the pilus unbinding rate k_{plane} , corresponding to k_{rupt} for pilus-pilus unbinding, is varied. The other parameters governing pilus-wall binding are assumed to be the same as for pilus-pilus interactions, see Tab. I. Experimentally, such wall properties can be realized, e.g., by coating hydrogel surfaces with pilin.

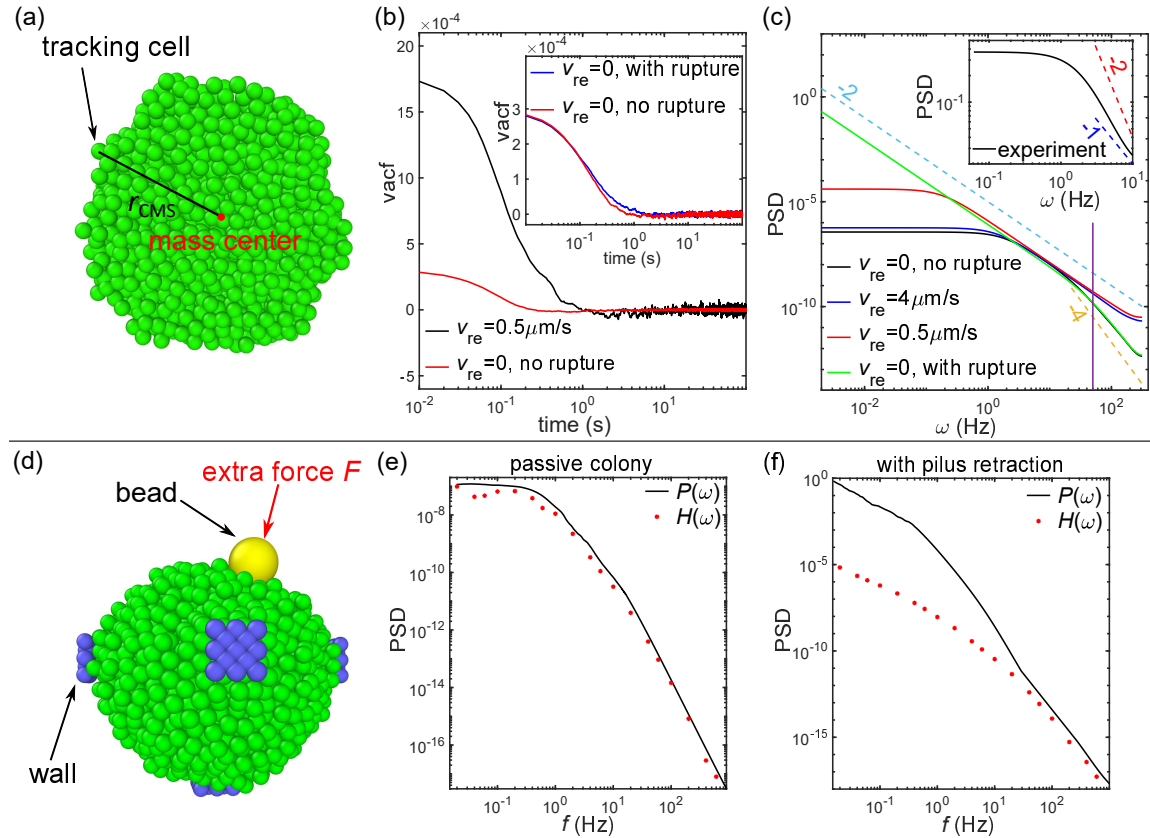


FIG. 5. (a) Simulated setup for quantifying boundary fluctuations by measuring the radial distance r_{CMS} between a fixed angular position on the surface and the colony center. (b) Active pilus retraction results in a slower decay of the velocity autocorrelation function (VACF) of the surface point. Inset: VACF of a colony grown with retraction-deficient cells. (c) Active pilus retraction produces a power spectral density of fluctuations characteristic for a visco-elastic material with an elastic response at low frequencies. Vertical line indicates frequencies above which simulations and experiments are not expected to match due to inertial effects. Inset: experimental data. (d) Simulation setup for mechanical perturbation of the colony shape. The colony is constrained between rigid walls and a bead is used to apply an external force onto the colony boundary. (e) Demonstration of the validity of the equilibrium fluctuation-response relationship for cells interaction with retraction-deficient pili forming permanent bonds. (f) Active pili result in deviations from equilibrium fluctuation-response relationship across the whole measurable frequency range and up to five orders of magnitude ($v_{\text{re}} = 0.5 \mu\text{m/s}$, $d_{\text{bind}} = 2.0 \mu\text{m}$)

Colonies growing upon a planar surface are shown in Fig. 6(a-c). If the dissociation rate constant of the pilus-wall bonds is smaller than the dissociation rate for pilus-pilus bonds, $k_{\text{plane}} \ll k_{\text{rupt}} = 10 \text{ 1/s}$, the colonies dissolve and the bacteria are evenly dispersed along the surface, see Fig. 6(a). For $k_{\text{plane}} \geq k_{\text{rupt}}$, the colonies assume rounded shapes that can still remain in loose contact with the surface, see Fig. 6(c). We also simulate the invasion of small channels by colonies, see Fig. 6(d-f). The qualitative features of this spreading of the colonies into channels are not entirely consistent with the notion of a passive wetting process. Moreover, we only observe significant channel invasion for colonies consisting of cells that can retract their pili and thereby generate forces actively.

IV. SUMMARY AND CONCLUDING REMARKS

The main purpose of this work is the establishment of an efficient computer simulation framework for modeling active, growing bacteria on different time- and length-scales. Bacterial cells are modeled with an algorithm akin to dissipative particle dynamics that is implemented in a dedicated package for a molecular-dynamics code. Parameter values are carefully chosen to allow comparison of the simulation results with experimental measurements. Using this program, we investigate different physical aspects of *N. gonorrhoeae* colonies, including growth dynamics, local ordering, and self-sorting of bacteria in colonies. Simulation results are in agreement with experimental data. We also propose a setup for measuring fluctuations in the colony shape and its response to external force. The simulations predict a strong, measurable violation of the equilibrium fluctuation-response relationship. Looking forward, we expect that future experimental and theoretical work on the non-equilibrium properties of bacterial colonies will generate insights that deepen our understanding of the emergent properties of active matter systems.

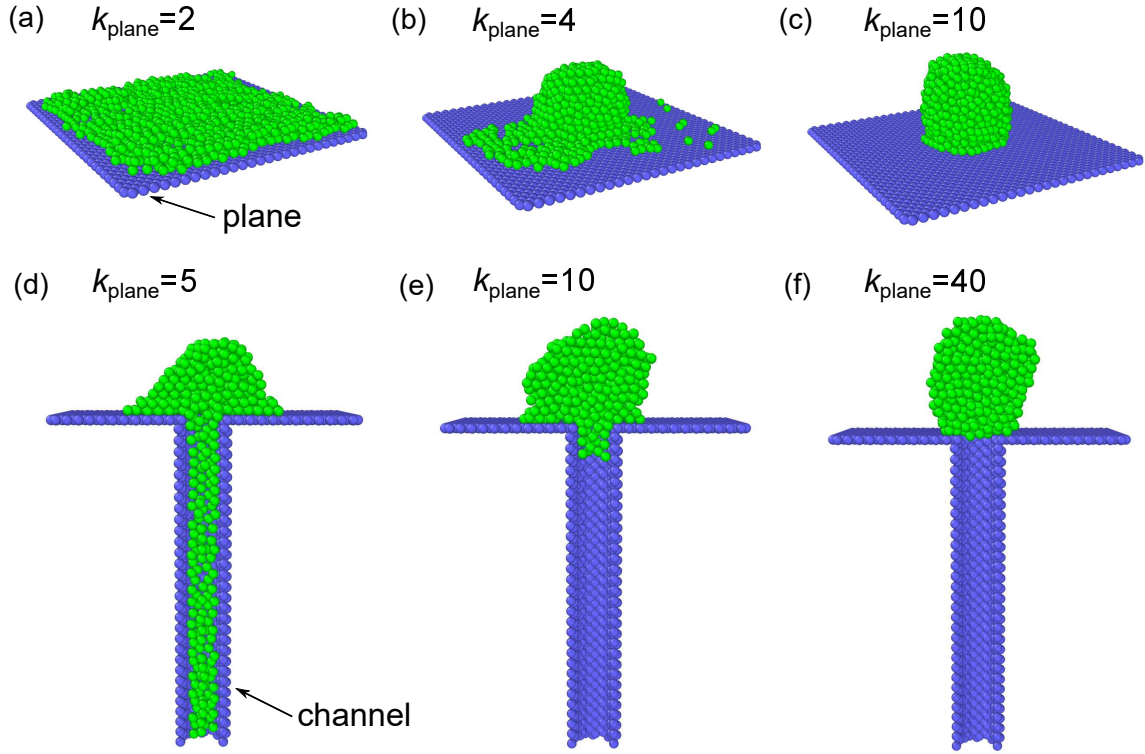


FIG. 6. Interaction of colonies with external boundaries. (a-c) Colonies on planar surfaces. Depending on the dissociation rate constant of pilus-surface bonds, k_{plane} , colonies undergo a partial or complete wetting transition. Pilus-substrate binding rates and rupture-forces are assumed to be those for pilus-pilus bonds. (d-f) Colonies initially positioned on top of a narrow channel can invade the channel if the pili-substrate bonds are strong, i.e., $k_{\text{plane}} < k_{\text{rupt}}$.

ACKNOWLEDGMENTS

KZ acknowledges kind support from the China Scholarship Council (CSC, No. 201804910439). Partial funding by the European Research Council is acknowledged

(BacForce, grant agreement No. 852585).

- [1] A. Welker, T. Cronenberg, R. Zöllner, C. Meel, K. Siewering, N. Bender, M. Hennes, E. R. Oldewurtel, and B. Maier, Molecular motors govern liquidlike ordering and fusion dynamics of bacterial colonies, *Phys. Rev. Lett.* **121**, 118102 (2018).
- [2] S. R. Balmuri, N. G. Waters, J. Hegemann, J. Kierfeld, and T. H. Niepa, Material properties of interfacial films of mucoid and nonmucoid *pseudomonas aeruginosa* isolates, *Acta Biomater.* **118**, 129 (2020).
- [3] L. Craig, K. T. Forest, and B. Maier, Type iv pili: dynamics, biophysics and functional consequences, *Nat. Rev. Microbiol.* **17**, 429 (2019).
- [4] R. Zöllner, T. Cronenberg, and B. Maier, Motor properties of pilt-independent type 4 pilus retraction in gonococci, *J. Bacteriol.* **201**, e00778 (2019).
- [5] R. Marathe, C. Meel, N. C. Schmidt, L. Dewenter, R. Kurre, L. Greune, M. A. Schmidt, M. J. Müller, R. Lipowsky, B. Maier, and S. Klumpp, Bacterial twitching motility is coordinated by a two-dimensional tug-of-war with directional memory, *Nat. Commun.* **5**, 1 (2014).
- [6] B. Maier, L. Potter, M. So, H. S. Seifert, and M. P. Sheetz, Single pilus motor forces exceed 100 pn, *Proc. Natl. Acad. Sci. U.S.A.* **99**, 16012 (2002).
- [7] J. M. Skerker and H. C. Berg, Direct observation of extension and retraction of type iv pili, *Proc. Natl. Acad. Sci. U.S.A.* **98**, 6901 (2001).
- [8] C. Holz, D. Opitz, L. Greune, R. Kurre, M. Koomey, M. A. Schmidt, and B. Maier, Multiple pilus motors cooperate for persistent bacterial movement in two dimensions, *Phys. Rev. Lett.* **104**, 178104 (2010).
- [9] W. Pönisch, C. A. Weber, G. Juckeland, N. Biais, and V. Zaburdaev, Multiscale modeling of bacterial colonies: how pili mediate the dynamics of single cells and

cellular aggregates, *New J. Phys.* **19**, 015003 (2017).

- [10] R. Kurre and B. Maier, Oxygen depletion triggers switching between discrete speed modes of gonococcal type iv pili, *Biophys. J.* **102**, 2556 (2012).
- [11] L. Dewenter, T. E. Volkmann, and B. Maier, Oxygen governs gonococcal microcolony stability by enhancing the interaction force between type iv pili, *Integr. Biol.* **7**, 1161 (2015).
- [12] J. Taktikos, Y. T. Lin, H. Stark, N. Biais, and V. Zaburdaev, Pili-induced clustering of *n. gonorrhoeae* bacteria, *PLoS One* **10**, e0137661 (2015).
- [13] R. Zöllner, T. Cronenberg, N. Kouzel, A. Welker, M. Koomey, and B. Maier, Type iv pilin post-translational modifications modulate material properties of bacterial colonies, *Biophys. J.* **116**, 938 (2019).
- [14] E. R. Oldewurtel, N. Kouzel, L. Dewenter, K. Henseler, and B. Maier, Differential interaction forces govern bacterial sorting in early biofilms, *eLife* **4**, e10811 (2015).
- [15] W. Pönisch, K. B. Eckenrode, K. Alzurqa, H. Nasrollahi, C. Weber, V. Zaburdaev, and N. Biais, Pili mediated intercellular forces shape heterogeneous bacterial microcolonies prior to multicellular differentiation, *Sci. Rep.* **8**, 1 (2018).
- [16] D. Bonazzi, V. L. Schiavo, S. Machata, I. Djafer-Cherif, P. Nivoit, V. Manriquez, H. Tanimoto, J. Husson, N. Henry, H. Chaté, *et al.*, Intermittent pili-mediated forces fluidize *neisseria meningitidis* aggregates promoting vascular colonization, *Cell* **174**, 143 (2018).
- [17] D. L. Higashi, S. W. Lee, A. Snyder, N. J. Weyand, A. Bakke, and M. So, Dynamics of *neisseria gonorrhoeae* attachment: microcolony development, cortical plaque formation, and cytoprotection, *Infect. Immun.* **75**, 4743 (2007).
- [18] U. Seifert, Stochastic thermodynamics, fluctuation theorems and molecular machines, *Rep. Prog. Phys.* **75**, 126001 (2012).

- [19] F. S. Gnesotto, F. Mura, J. Gladrow, and C. P. Broedersz, Broken detailed balance and non-equilibrium dynamics in living systems: a review, *Rep. Prog. Phys.* **81**, 066601 (2018).
- [20] T. Harada and S.-i. Sasa, Equality connecting energy dissipation with a violation of the fluctuation-response relation, *Phys. Rev. Lett.* **95**, 130602 (2005).
- [21] D. Mizuno, C. Tardin, C. F. Schmidt, and F. C. MacKintosh, Nonequilibrium mechanics of active cytoskeletal networks, *Science* **315**, 370 (2007).
- [22] R. R. Netz, Fluctuation-dissipation relation and stationary distribution of an exactly solvable many-particle model for active biomatter far from equilibrium, *J. Chem. Phys.* **148**, 185101 (2018).
- [23] H.-S. Kuan, W. Pönisch, F. Jülicher, and V. Zaburdaev, Continuum theory of active phase separation in cellular aggregates, *Phys. Rev. Lett.* **126**, 018102 (2021).
- [24] J. Ranft, M. Basan, J. Elgeti, J.-F. Joanny, J. Prost, and F. Jülicher, Fluidization of tissues by cell division and apoptosis, *Proc. Natl. Acad. Sci. U. S. A.* **107**, 20863 (2010).
- [25] N. Podewitz, M. Delarue, and J. Elgeti, Tissue homeostasis: A tensile state, *Europhys. Lett.* **109**, 58005 (2015).
- [26] S. Plimpton, Fast parallel algorithms for short-range molecular dynamics, *J. Comput. Phys.* **117**, 1 (1995).
- [27] A. Stukowski, Visualization and analysis of atomistic simulation data with ovito—the open visualization tool, *Modell. Simul. Mater. Sci. Eng.* **18**, 015012 (2009).
- [28] A. Beaussart, A. E. Baker, S. L. Kuchma, S. El-Kirat-Chatel, G. A. O’Toole, and Y. F. Dufrêne, Nanoscale adhesion forces of *pseudomonas aeruginosa* type iv pili, *Acs Nano* **8**, 10723 (2014).
- [29] A. Welker, M. Hennes, N. Bender, T. Cronenberg, G. Schneider, and B. Maier, Spatio-temporal dynamics of growth and death within spherical bacterial colonies, *bioRxiv*

(2021).

- [30] K. Younge, C. Christenson, A. Bohara, J. Crnkovic, and P. Saulnier, A model system for examining the radial distribution function, *Am. J. Phys.* **72**, 1247 (2004).
- [31] B. A. Kopera and M. Retsch, Computing the 3d radial distribution function from particle positions: an advanced analytic approach, *Anal. Chem.* **90**, 13909 (2018).
- [32] T. Cronenberg, M. Hennes, I. Wielert, and B. Maier, Antibiotics modulate attractive interactions in bacterial colonies affecting survivability under combined treatment, *PLoS Pathog.* **17**, e1009251 (2021).